

Review

Novel Electronic State and Superconductivity in the Electron-Doped High- T_c T'-Superconductors

Tadashi Adachi ^{1,*}, Takayuki Kawamata ² and Yoji Koike ²¹ Department of Engineering and Applied Sciences, Sophia University, Tokyo 102-8554, Japan² Department of Applied Physics, Graduate School of Engineering, Tohoku University, Sendai 980-8579, Japan; tkawamata@teion.apph.tohoku.ac.jp (T.K.); koike@teion.apph.tohoku.ac.jp (Y.K.)

* Correspondence: t-adachi@sophia.ac.jp; Tel.: +81-3-3238-3402

Received: 28 April 2017; Accepted: 27 June 2017; Published: 4 July 2017

Abstract: In this review article, we show our recent results relating to the undoped (Ce-free) superconductivity in the electron-doped high- T_c cuprates with the so-called T' structure. For an introduction, we briefly mention the characteristics of the electron-doped T'-cuprates, including the reduction annealing, conventional phase diagram and undoped superconductivity. Then, our transport and magnetic results and results relating to the superconducting pairing symmetry of the undoped and underdoped T'-cuprates are shown. Collaborating spectroscopic and nuclear magnetic resonance results are also shown briefly. It has been found that, through the reduction annealing, a strongly localized state of carriers accompanied by an antiferromagnetic pseudogap in the as-grown samples changes to a metallic and superconducting state with a short-range magnetic order in the reduced superconducting samples. The formation of the short-range magnetic order due to a very small amount of excess oxygen in the reduced superconducting samples suggests that the T'-cuprates exhibiting the undoped superconductivity in the parent compounds are regarded as strongly correlated electron systems, as well as the hole-doped high- T_c cuprates. We show our proposed electronic structure model to understand the undoped superconductivity. Finally, unsolved future issues of the T'-cuprates are discussed.

Keywords: electron-doped high- T_c cuprate; undoped (Ce-free) superconductivity; reduction annealing; transport property; muon spin relaxation; novel electronic structure model

1. Introduction

In the past three decades, cuprates exhibiting high-temperature superconductivity have been intensively studied. The superconducting (SC) transition temperature $T_c \sim 134$ K [1] in the Hg-1223 cuprate is the highest among all SC materials at ambient pressure. Although new high- T_c superconductors of iron arsenides with the maximum T_c of ~ 55 K [2] and of sulfur hydrides with $T_c \sim 203$ K at 200 GPa [3] have been observed, the cuprates have been standing for potential materials of both exotic physics and future applications. All series of high- T_c cuprates, La-214, Y-123, Bi-2212, etc., have the parent compounds, which are antiferromagnetic (AF) Mott insulators. As shown in the phase diagram of Figure 1a, in the hole-doped cuprates, doping of hole carriers into the parent compound destroys an AF order quickly, and then, the superconductivity appears. With increasing hole doping, T_c is raised in the underdoped regime and exhibits the maximum in the optimally doped regime. With further doping, T_c turns into a decrease in the overdoped regime, and finally, the superconductivity disappears in the heavily-overdoped regime where the system becomes a metal. Comprehensive neutron scattering [4] and muon spin relaxation (μ SR) [5–9] experiments have uncovered AF fluctuations in the SC doping regime, suggesting that AF fluctuations are a glue to form SC electron pairs. In the non-SC heavily-overdoped regime, recent theories [10–12] and experiments [13,14] have suggested the existence of ferromagnetic fluctuations of itinerant carriers.

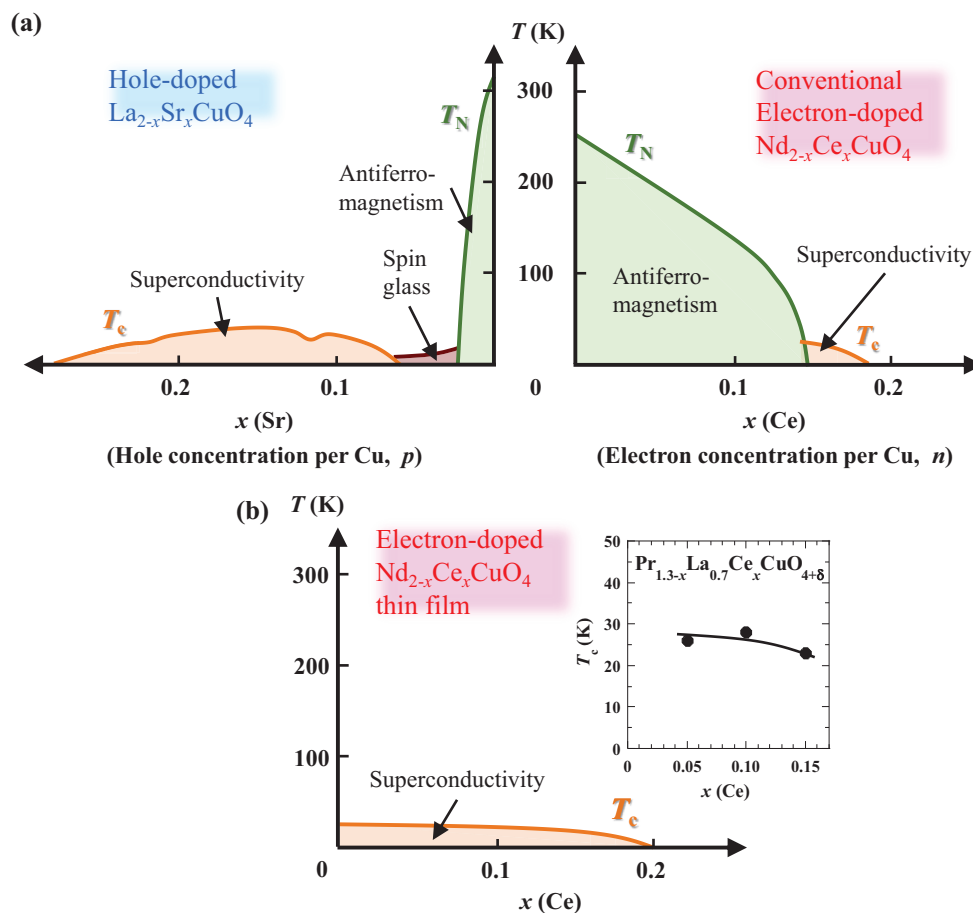


Figure 1. Phase diagrams of (a) the hole-doped and conventional electron-doped high- T_c cuprates and (b) the electron-doped cuprates newly proposed in thin films. The inset of (b) is the Ce concentration dependence of T_c in single crystals of electron-doped $\text{Pr}_{1.3-x}\text{La}_{0.7}\text{Ce}_x\text{CuO}_{4+\delta}$.

Electron-doped high- T_c cuprates were first discovered by Tokura et al. in 1989 [15]. Pronounced features different from those in the hole-doped cuprates are not only the electron carrier, but also the reduction annealing, which is absolutely essential to obtain the superconductivity in the electron-doped cuprates. The phase diagram depicted by the normally reduced samples is shown in Figure 1a, which roughly resembles that of the hole-doped cuprates. The doping of electrons into the parent compounds weakens the AF order, but the AF order is maintained around the optimally doped regime. The superconductivity with the maximum T_c appears around the optimally doped regime and is monotonically suppressed with over-doping. Since AF fluctuations were observed around the optimally doped regime [16], the electron pairing mediated by AF fluctuations has been believed to be the case also in the electron-doped cuprates. In 2005, a surprising result was obtained in thin films of the electron-doped cuprates with the Nd_2CuO_4 -type structure (the so-called T' structure), in which the superconductivity appears without electron doping [17]. Following observations of the undoped (Ce-free) superconductivity in the parent compounds [18,19] and the suggestion of a new phase diagram shown in Figure 1b [20] opened a new era of research in the high- T_c superconductivity. Yet to date, the mechanism of the undoped superconductivity is unclear.

In this review article, we show our recent results relating to the undoped superconductivity in the T'-cuprates [21–23]. First, we present the characteristics of the electron-doped T'-cuprates including the reduction annealing, conventional phase diagram and undoped superconductivity. The next three sections consist of our transport and magnetic results and results relating to the SC pairing symmetry. Collaborating spectroscopic and nuclear magnetic resonance (NMR) results

are also shown briefly. Then, we discuss our proposed electronic structure model to understand the undoped superconductivity. In the final section, unsolved future issues of the T'-cuprates are discussed. Note that there are already excellent and complete reviews on the materials and physics focusing on the conventional electron-doped cuprates [24,25].

2. Electron-Doped T'-Cuprate

Electron-doped T'-cuprates were discovered in $\text{Nd}_{2-x}\text{Ce}_x\text{CuO}_4$ [15]. This class of materials are expressed as RE_2CuO_4 ($\text{RE} = \text{Pr}, \text{Nd}, \text{Sm}, \text{Eu}$) with the T' structure. The electron doping is achieved by the substitution of the tetravalent Ce^{4+} for the trivalent RE^{3+} . The T' structure consists of the CuO_2 plane and fluorite-type blocking layer. Because as-grown T'-samples are insulating and AF, the reduction annealing for the as-grown T'-cuprates is indispensable to obtain superconductivity. One of the unsolved puzzles for the T'-cuprates is the exact mechanism of the reduction process. To date, there are mainly two candidate mechanisms for this puzzle. One is the removal of excess oxygen from the as-grown sample, which is mostly believed from the early stage of the research of the T'-cuprates. This idea originated from early neutron-diffraction experiments in $\text{Nd}_{2-x}\text{Ce}_x\text{CuO}_4$ [26,27]. Because of the size mismatch between the CuO_2 plane and blocking layer, excess oxygen tends to be included right above Cu, resulting in the shrinkage of the blocking layer in the *ab*-plane. Since the excess oxygen is understood to induce disorder of the electrostatic potential in the CuO_2 plane, electron pairs are destroyed, and the system shows no SC behaviors [28]. Therefore, the removal of excess oxygen from the as-grown sample is crucial for the appearance of superconductivity and the investigation of intrinsic properties of the T'-cuprates. The other is the Cu-vacancy scenario proposed by neutron and X-ray diffraction studies in $\text{Nd}_{2-x}\text{Ce}_x\text{CuO}_4$ [29] and $\text{Pr}_{1-x}\text{LaCe}_x\text{CuO}_4$ [30]. The diffraction experiments found that (i) the occupancy at the Cu site is imperfect (perfect) in the as-grown (reduced) samples and (ii) the so-called secondary phase of RE_2O_3 appears (disappears) through the reduction (oxidation) annealing, both of which are reversible processes through the reduction (oxidation) annealing. Therefore, the role of the reduction annealing is to fill up Cu deficiencies in the as-grown samples where Cu deficiencies are regarded as causing the pair breaking. The secondary phase was precisely investigated in $\text{Nd}_{2-x}\text{Ce}_x\text{CuO}_4$ [31].

The phase diagram of T'-cuprates was first obtained by μSR in $\text{Nd}_{2-x}\text{Ce}_x\text{CuO}_4$ (Figure 1a) [32] and later in $\text{Pr}_{1-x}\text{LaCe}_x\text{CuO}_4$ [33]. The AF phase expands up to the optimally doped regime, and the optimal superconductivity suddenly sets in at the same time of the suppression of the AF order. In detail, both the superconductivity and AF order coexist around the boundary of two phases. With over-doping, T_c monotonically decreases and disappears around the region of the solubility limit of Ce into the T'-structure. Neutron-scattering experiments in $\text{Nd}_{2-x}\text{Ce}_x\text{CuO}_4$ around the optimally doped regime of $x = 0.15$ revealed commensurate AF fluctuations [16]. This is in sharp contrast to incommensurate AF fluctuations [4] or stripe fluctuations [34] observed in the hole-doped cuprates. Following neutron-scattering experiments in $\text{Pr}_{1-x}\text{LaCe}_x\text{CuO}_4$ [35] uncovered that commensurate AF fluctuations existed also in the overdoped regime and that both the spin stiffness and relaxation rate of AF fluctuations decreased toward the end point of superconductivity in the heavily overdoped regime. These suggest the intimate relation between the superconductivity and AF fluctuations in the T'-cuprates, as well as in the hole-doped cuprates.

In 1995, Brinkmann et al. reported pioneering results, which later led to the discovery of undoped (Ce-free) superconductivity [36]. They tried to expand the SC regime deeply into the AF underdoped regime in the phase diagram by improving the reduction process. A thin single crystal of $\text{Pr}_{2-x}\text{Ce}_x\text{CuO}_4$ was sandwiched by polycrystalline pellets of the same component to protect the surface of the crystal and annealed at a higher temperature of 1080 °C for a longer time than in the conventional annealing. They observed the superconductivity down to $x = 0.04$ in the underdoped regime. Moreover, T_c gradually increased with decreasing doping from the optimally doped regime. They suggested that the superconductivity in underdoped $\text{Pr}_{2-x}\text{Ce}_x\text{CuO}_4$ was a product of the appropriate reduction of excess oxygen. Then, one would think of lower doping regime than $x = 0.04$,

namely whether Mott insulators like the hole-doped cuprates or superconductivity down to the parent compound.

Ten years later, a surprising result was obtained by Tsukada et al. in T' thin films of Ce-free $\text{La}_{2-y}\text{RE}_y\text{CuO}_4$ ($\text{RE} = \text{Y, Lu, Sm, Eu, Gd, Tb}$) in which the superconductivity appears without Ce substitution (electron doping) [17]. Subsequent systematic investigation by the same group using $\text{Nd}_{2-x}\text{Ce}_x\text{CuO}_4$ thin films uncovered that T_c of ~ 28 K in the parent compound of $x = 0$ decreased monotonically with increasing x and disappeared at $x \sim 0.20$ (Figure 1b) [20]. These findings were suggested to be due to the removal of excess oxygen from the as-grown thin films more effectively than that ever reported. Their unique procedure of the reduction annealing called two-step annealing was mentioned in the literature [37]. At the first step, the as-grown thin films were annealed at a high temperature in an intermediate oxygen pressure of $\sim 10^2$ Pa. In this process, they insisted based on the increasing ab -plane electrical resistivity ρ_{ab} and unchanged c -axis length that oxygen in the CuO_2 plane was mainly removed, and excess oxygen was not. At the second step, the thin films were further annealed at a low temperature in a low oxygen pressure of $\sim 10^{-5}$ Pa. In this process, they insisted based on the decreasing ρ_{ab} and c -axis length that excess oxygen moved to the oxygen-defect site in the CuO_2 plane, and the superconductivity was realized. In fact, optical studies of the SC thin film of Pr_2CuO_x with $x \simeq 4$ have revealed a Drude-like peak centered at zero frequency, suggesting a metallic state of the SC parent compound [38]. These results give us the following messages: (i) the newly-proposed phase diagram without the AF phase is seemingly different from the conventional one; and (ii) the AF Mott insulating state is not a starting point of the superconductivity in the T' -cuprates. The superconductivity in the parent compounds of the T' -cuprates was also confirmed using polycrystalline samples of Ce-free $\text{La}_{2-y}\text{Sm}_y\text{CuO}_4$ [18] and Ce-free $\text{La}_{1.8}\text{Eu}_{0.2}\text{CuO}_4$ [19], while it has not yet been confirmed in single crystals of the parent compound.

From the theoretical viewpoint, the undoped (Ce-free) superconductivity in the parent compounds might be explained by the early local density energy band calculation in $\text{Nd}_{2-x}\text{Ce}_x\text{CuO}_4$ [39] where the system was a simple band metal without electron correlation. On the assumption of the moderate electron correlation, the half-filled-band Hubbard model consisting of doublons and holons predicted the superconductivity in the parent compound [40]. Under the strong electron correlation generating the Mott-Hubbard gap between the upper Hubbard band (UHB) and the lower Hubbard band (LHB) of the Cu $3d_{x^2-y^2}$ orbital, calculations based on the local density approximation (LDA) combined with the dynamical mean-field theory (DMFT) revealed the possibility of the closing of the so-called charge-transfer (CT) gap between UHB of the Cu $3d_{x^2-y^2}$ orbital and the O $2p$ band observed in the hole-doped cuprates [41,42]. That is, both metallic and SC states were suggested to appear by eliminating the AF order in the parent compounds of the T' -cuprates. The recent calculation of a two-particle self-consistent analysis using the three-band model [43] revealed a monotonic decrease in T_c with electron doping, which is consistent with the experimental observation shown in Figure 1b [20].

The undoped (Ce-free) superconductivity challenges the long-thought understanding that the parent compounds of the high- T_c cuprates are AF Mott insulators. To understand the mechanism of the undoped superconductivity, it is extremely important to clarify the evolution of the electronic state through the reduction process, for which the detailed investigation using single crystals is necessary. One of critical questions is whether or not the undoped superconductivity in the T' -cuprates appears based on the strong electron correlation. To answer this issue, it is significant to investigate the Cu-spin correlation, because localized Cu spins in LHB of the Cu $3d_{x^2-y^2}$ orbital are generated and expected to correlate with one another in the case of the strong electron correlation. To attain these aims, we used T' single crystals of Ce-underdoped $\text{Pr}_{1.3-x}\text{La}_{0.7}\text{Ce}_x\text{CuO}_{4+\delta}$ with $x = 0.10$ and undoped (Ce-free) SC samples of $\text{La}_{1.8}\text{Eu}_{0.2}\text{CuO}_{4+\delta}$. In the next section, we start from the preparation of single crystals and the improved reduction annealing in $\text{Pr}_{1.3-x}\text{La}_{0.7}\text{Ce}_x\text{CuO}_{4+\delta}$.

3. Evolution of the Electronic State through the Reduction Annealing

Single crystals of Ce-underdoped $\text{Pr}_{1.3-x}\text{La}_{0.7}\text{Ce}_x\text{CuO}_{4+\delta}$ with $x = 0.10$ were grown by the traveling-solvent floating-zone method [33,44]. In order to reduce excess oxygen in the as-grown crystals, we grew single crystals in air atmosphere, which is at a lower partial pressure of oxygen than formerly reported [33,45]. The composition of as-grown crystals was determined by the inductively-coupled plasma (ICP) analysis to be $\text{Pr}_{1.17(1)}\text{La}_{0.73(1)}\text{Ce}_{0.10(1)}\text{Cu}_{1.00(1)}\text{O}_4$, which is close to the nominal composition. For the as-grown crystals, we performed the reduction annealing in vacuum of $\sim 10^{-4}$ Pa for 24 h at various temperatures. In order to protect the surface of crystals during the annealing, the as-grown crystals were covered with polycrystalline powders having the same composition (protect annealing). This is an improved technique of the Brinkmann's [36]. From the iodometric titration, the oxygen content was confirmed to be reduced by 0.03(1) through the reduction annealing for $\text{Pr}_{1.3-x}\text{La}_{0.7}\text{Ce}_x\text{CuO}_{4+\delta}$ with $x = 0.10$. Moreover, through the reduction annealing, the c -axis lengths estimated from the X-ray diffraction measurements were reduced by 0.028(1) Å for $\text{Pr}_{1.3-x}\text{La}_{0.7}\text{Ce}_x\text{CuO}_{4+\delta}$ with $x = 0.10$, suggesting the removal of excess oxygen from the as-grown samples. The scanning electron microscope also revealed that, in the reduced SC crystal, neither Cu metals nor rare-earth oxides were observed. Therefore, both the absence of Cu deficiency within the error of ICP and the oxygen reduction through the annealing suggest that the Cu deficiency model is not applicable to the present samples. Polycrystalline samples of undoped (Ce-free) $\text{La}_{1.8}\text{Eu}_{0.2}\text{CuO}_{4+\delta}$ were prepared by a low-temperature technique using CaH_2 as a reductant and the subsequent annealing. The SC samples were obtained through the reduction annealing at 700 °C for 24 h in vacuum. Details have been described in the literature [19].

Figure 2 shows the temperature dependence of the magnetic susceptibility of $\text{Pr}_{1.3-x}\text{La}_{0.7}\text{Ce}_x\text{CuO}_{4+\delta}$ with $x = 0.10$ and $\text{La}_{1.8}\text{Eu}_{0.2}\text{CuO}_{4+\delta}$. For $\text{Pr}_{1.3-x}\text{La}_{0.7}\text{Ce}_x\text{CuO}_{4+\delta}$, the Meissner diamagnetism appears in the 750 °C-reduced crystal, and the relatively sharp SC transition with the onset of ~ 27 K is observed in the 800 °C-reduced crystal. Formerly, Sun et al. reported from transport properties of reduced single crystals of $\text{Pr}_{1.3-x}\text{La}_{0.7}\text{Ce}_x\text{CuO}_{4+\delta}$ through the annealing in Ar that the crystals with $x \leq 0.10$ are non-SC [46]. The present successful observation of bulk superconductivity in $\text{Pr}_{1.3-x}\text{La}_{0.7}\text{Ce}_x\text{CuO}_{4+\delta}$ with $x = 0.10$ suggests that the excess oxygen is effectively removed from the as-grown crystal through the protect annealing in vacuum at lower temperatures than in the conventional annealing. The $\text{La}_{1.8}\text{Eu}_{0.2}\text{CuO}_{4+\delta}$ sample also shows the bulk Meissner diamagnetism below ~ 15 K, which is almost the same as that formerly reported [19].

The temperature dependence of ρ_{ab} in $\text{Pr}_{1.3-x}\text{La}_{0.7}\text{Ce}_x\text{CuO}_{4+\delta}$ with $x = 0.10$ exhibits characteristic behaviors depending on the reduction condition, as shown in Figure 3a. The as-grown crystal shows semiconducting temperature dependence and no trace of superconductivity. For the 650 °C-reduced crystal, ρ_{ab} is semiconducting at high temperatures, while a drop of ρ_{ab} is observed below ~ 7 K due to the SC transition. The drastic decrease in ρ_{ab} is observed in the 750 °C- and 800 °C-reduced crystals in which the bulk superconductivity appears. Both crystals show a metallic behavior at high temperatures and an upturn at low temperatures, followed by the SC transition. In the normal state below ~ 50 K, ρ_{ab} exhibits $\log T$ dependence. This behavior, as well as the saturation of ρ_{ab} in the magnetic field and negative magnetoresistance [21] is most likely due to the Kondo effect [47]. The present evolution of ρ_{ab} through the reduction annealing suggests that the strongly localized state of carriers in the as-grown crystal changes to a metallic state with the Kondo effect in $\text{Pr}_{1.3-x}\text{La}_{0.7}\text{Ce}_x\text{CuO}_{4+\delta}$ with $x = 0.10$.

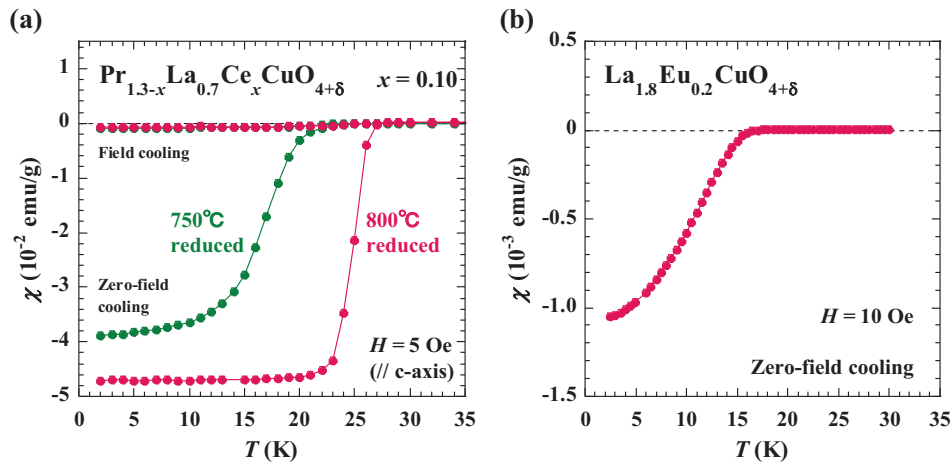


Figure 2. Temperature dependence of the magnetic susceptibility of (a) Ce-underdoped $\text{Pr}_{1.3-x}\text{La}_{0.7}\text{Ce}_x\text{CuO}_{4+\delta}$ with $x = 0.10$ and (b) undoped (Ce-free) $\text{La}_{1.8}\text{Eu}_{0.2}\text{CuO}_{4+\delta}$.

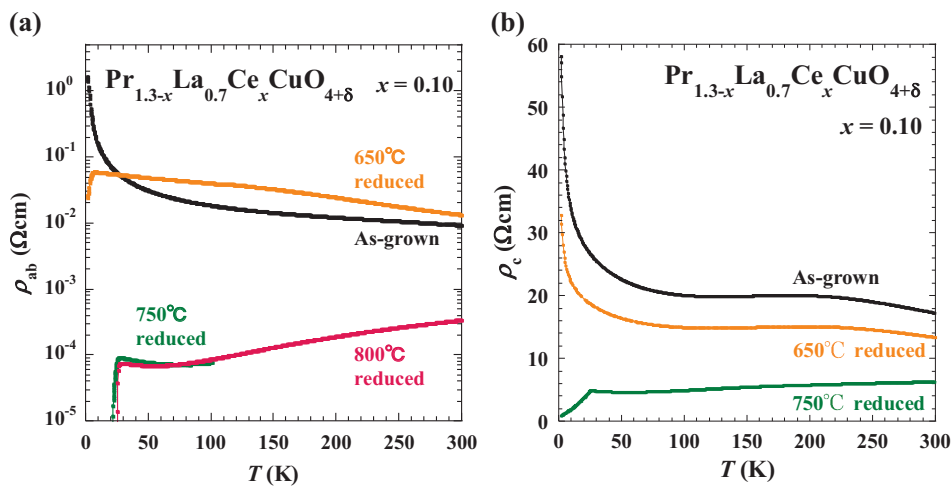


Figure 3. Temperature dependence of the (a) *ab*-plane and (b) *c*-axis electrical resistivity of Ce-underdoped $\text{Pr}_{1.3-x}\text{La}_{0.7}\text{Ce}_x\text{CuO}_{4+\delta}$ with $x = 0.10$ in various annealing conditions.

Figure 3b shows the temperature dependence of the *c*-axis resistivity ρ_c for $\text{Pr}_{1.3-x}\text{La}_{0.7}\text{Ce}_x\text{CuO}_{4+\delta}$ with $x = 0.10$. For the as-grown and 650 °C-reduced crystals, a hump is observed at ~ 200 K, which is similar to that observed in $\text{Nd}_{2-x}\text{Ce}_x\text{CuO}_4$ with $x < 0.14$ [45] and $\text{Pr}_{1.3-x}\text{La}_{0.7}\text{Ce}_x\text{CuO}_{4+\delta}$ with $x \leq 0.03$ [46] and due to the opening of an AF pseudogap. For the 750 °C-reduced crystal, on the contrary, a simple metallic behavior without hump is observed, which resembles the behavior of ρ_c in SC $\text{Nd}_{2-x}\text{Ce}_x\text{CuO}_4$ with $x = 0.15$ [45]. Therefore, it is inferred that the AF pseudogap disappears in the 750 °C-reduced SC crystal.

The electronic state of $\text{Pr}_{1.3-x}\text{La}_{0.7}\text{Ce}_x\text{CuO}_{4+\delta}$ was further investigated by the angle-resolved photoemission spectroscopy (ARPES) by Horio et al. using our as-grown and reduced single crystals, as shown in Figure 4 [48]. For the as-grown and 650 °C-reduced crystals, the AF pseudogap is clearly observed around the hot spots, namely, crossing points of the Fermi surface with the AF Brillouin zone boundary. For the 800 °C-reduced crystal, on the contrary, the sharp quasi-particle peaks are observed on the entire Fermi surface without the signature of the AF pseudogap unlike the previous works [49,50]. These results are consistent with the ρ_c results in Figure 3b and indicate the dramatic reduction of the AF correlation length and/or of magnetic moments in the 800 °C-reduced crystal. The quasi-particle peaks around the anti-nodal region are broader than those around the nodal region,

suggesting the strong scattering of quasiparticles by the AF fluctuations and/or charge fluctuations in relation to the recent observation of the charge order in $\text{Nd}_{2-x}\text{Ce}_x\text{CuO}_4$ [51].

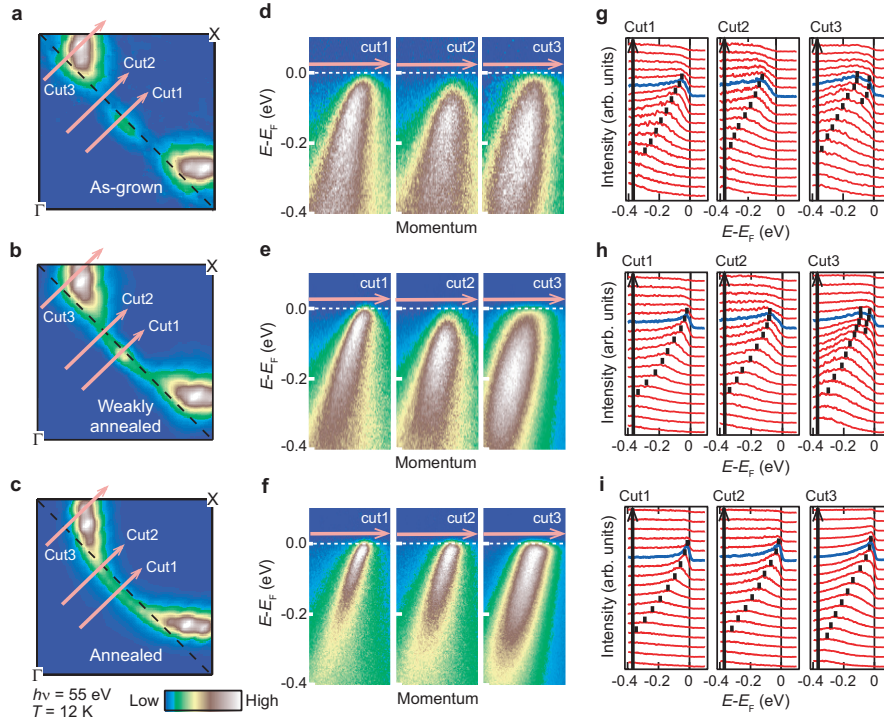


Figure 4. (a–c) Fermi-surface mappings of as-grown, 650 °C-reduced and 800 °C-reduced crystals of Ce-underdoped $\text{Pr}_{1.3-x}\text{La}_{0.7}\text{Ce}_x\text{CuO}_{4+\delta}$ with $x = 0.10$, respectively. The intensities at the hot spots, the crossing points of the Fermi surface with the AF Brillouin zone boundary, are suppressed in the as-grown and 650 °C-reduced crystals, while those are fully recovered in the 800 °C-reduced crystal. (d–f) Intensity plots in the energy-momentum space for each crystal along each cut indicated in (a–c). (g–i) Energy-distribution curves plotted for each cut. Blue energy-distribution curves are taken at positions of the Fermi wavenumber. Peak positions are marked by vertical bars. Quoted from [48].

The Hall effect of the electron-doped T'-cuprates is highly informative. Thin-film studies in $\text{Pr}_{2-x}\text{Ce}_x\text{CuO}_4$ reduced in the conventional annealing revealed that the Hall coefficient R_H was negative in the underdoped regime and increased with increasing x , followed by the sign change of R_H at $x \sim 0.17$ [52]. Moreover, the Hall resistivity ρ_{xy} exhibited a nonlinear behavior in the magnetic field in $\text{Pr}_{2-x}\text{Ce}_x\text{CuO}_4$ thin films [53]. Our results of ρ_{xy} in $\text{Pr}_{1.3-x}\text{La}_{0.7}\text{Ce}_x\text{CuO}_{4+\delta}$ with $x = 0.10$ also revealed a nonlinear behavior in the magnetic field. These suggest that multiple carriers (most likely electrons and holes) reside in the T'-cuprates. The existence of multiple carriers of electrons and holes has also been suggested from NMR in single crystals of $\text{Nd}_{2-x}\text{Ce}_x\text{CuO}_4$ and $\text{Pr}_{2-x}\text{Ce}_x\text{CuO}_4$ [54]. Note that the undoped SC thin films exhibit positive R_H in the ground state, suggesting the existence of predominant hole-like carriers [37].

4. Relationship between Cu-Spin Correlation and Superconductivity

For the detailed investigation of the Cu-spin correlation, we used the μSR technique which is highly sensitive to the local magnetism in a sample and has an advantage to distinguish between a long-range and short-range magnetic order. Zero-field (ZF) and longitudinal-field (LF) μSR measurements of $\text{Pr}_{1.3-x}\text{La}_{0.7}\text{Ce}_x\text{CuO}_{4+\delta}$ with $x = 0.10$ and $\text{La}_{1.8}\text{Eu}_{0.2}\text{CuO}_{4+\delta}$ were performed using a pulsed positive muon beam at the Material and Life Science Experimental Facility at J-PARC in Japan and using a continuous positive muon beam at the Paul-Scherrer Institute (PSI) in Switzerland, respectively.

Figure 5a,b show the ZF- μ SR time spectra of as-grown non-SC and 700 °C-reduced SC samples of $\text{La}_{1.8}\text{Eu}_{0.2}\text{CuO}_{4+\delta}$, respectively [22]. For both samples, Gaussian-like slow depolarizations due to nuclear dipole fields are observed at high temperatures, indicating a paramagnetic state of Cu spins. With decreasing temperature, fast depolarizations of muon spins are observed, suggesting the development of the Cu-spin correlation. For the as-grown sample, clear muon-spin precessions appear at low temperatures, indicating the formation of a long-range magnetic order. For the reduced SC sample, the spectrum consists of a fast depolarization without precession and a following time-independent behavior above 1 μs , which is typical of a short-range magnetically ordered state. In the LF- μ SR spectra at 1.6 K shown in Figure 5c [22], a parallel shift up with LF indicates the formation of a static magnetically ordered state in ZF. In $\text{Pr}_{1.3-x}\text{La}_{0.7}\text{Ce}_x\text{CuO}_{4+\delta}$ with $x = 0.10$, the as-grown non-SC crystal exhibits muon-spin precessions at low temperatures as shown in Figure 5d [22]. The spectra of the 800 °C-reduced SC crystal in Figure 5e [22] show both fast and slow depolarizations without muon-spin precession at 3 K. The LF- μ SR spectra at 10 K shown in Figure 5f [22] reveal a parallel shift as well as a slow depolarization with LF, suggesting the existence of both a short-range magnetic order and fluctuating Cu spins. These results indicate the coexisting state of the superconductivity and the short-range magnetic order in both $\text{La}_{1.8}\text{Eu}_{0.2}\text{CuO}_{4+\delta}$ and $\text{Pr}_{1.3-x}\text{La}_{0.7}\text{Ce}_x\text{CuO}_{4+\delta}$ with $x = 0.10$. Note that μ SR results of the undoped (Ce-free) thin film of $\text{La}_{2-x}\text{Y}_x\text{CuO}_{4+\delta}$ have shown the development of the Cu-spin correlation at low temperatures [55].

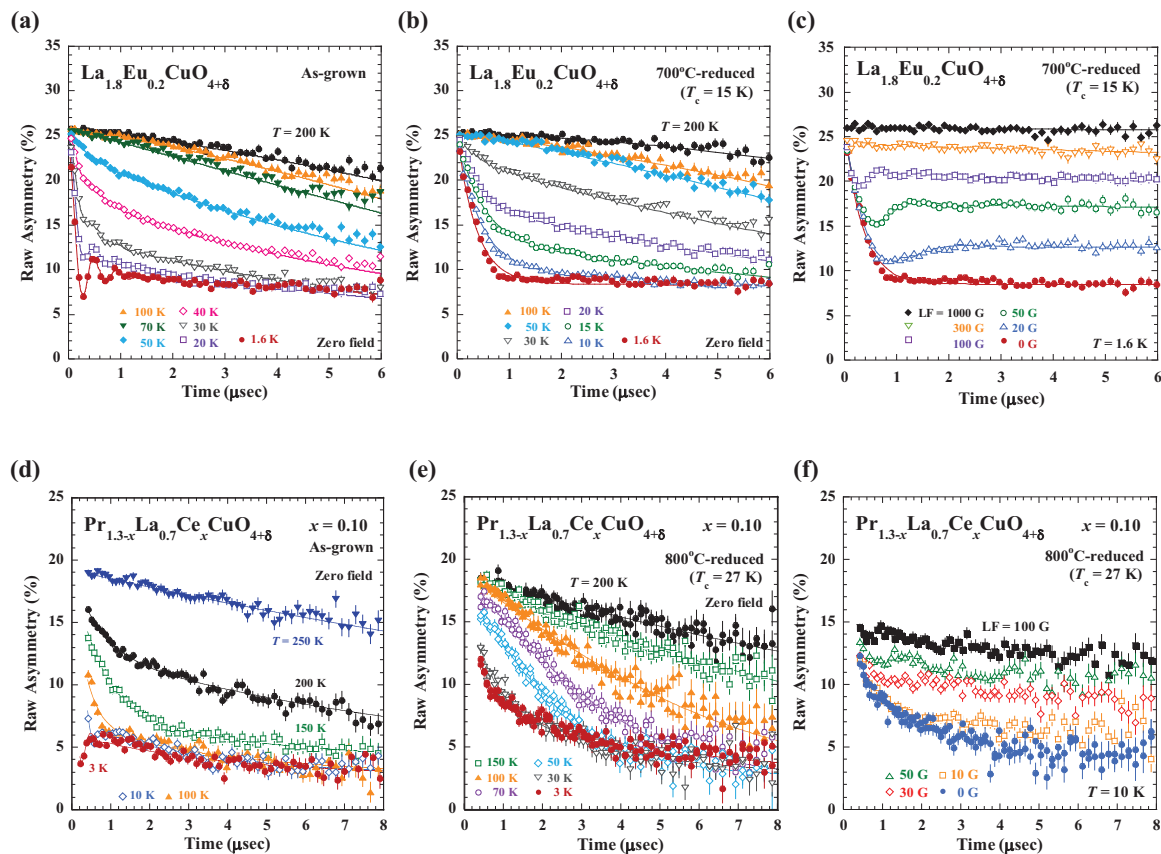


Figure 5. Zero-field (ZF) and longitudinal-field (LF) μ SR time spectra of undoped (Ce-free) and Ce-underdoped T'-cuprates [22]. (a,b) ZF- μ SR time spectra of as-grown non-SC and 700 °C-reduced SC samples of undoped (Ce-free) $\text{La}_{1.8}\text{Eu}_{0.2}\text{CuO}_{4+\delta}$; (c) LF- μ SR time spectra at 1.6 K of 700 °C-reduced SC samples of undoped $\text{La}_{1.8}\text{Eu}_{0.2}\text{CuO}_{4+\delta}$; (d,e) ZF- μ SR time spectra of as-grown non-SC and 800 °C-reduced SC crystals of Ce-underdoped $\text{Pr}_{1.3-x}\text{La}_{0.7}\text{Ce}_x\text{CuO}_{4+\delta}$ with $x = 0.10$; (f) LF- μ SR time spectra at 10 K of 800 °C-reduced SC crystal of $\text{Pr}_{1.3-x}\text{La}_{0.7}\text{Ce}_x\text{CuO}_{4+\delta}$ with $x = 0.10$. Solid lines in (a–e) indicate the best-fit results using the analysis function described in the literature.

The analysis of volume fractions of SC and short-range magnetically ordered regions leads to the detailed information on the electronic state in the T'-cuprates. The magnetic volume fractions were estimated from the μ SR results [22]. For the reduced SC $\text{La}_{1.8}\text{Eu}_{0.2}\text{CuO}_{4+\delta}$, the volume fraction of the short-range magnetically ordered region is almost 100% in the ground state. As the SC volume fraction is estimated from the Meissner fraction to be above 15%, both the SC and short-range magnetically ordered regions coexist in the sample. For the reduced SC $\text{Pr}_{1.3-x}\text{La}_{0.7}\text{Ce}_x\text{CuO}_{4+\delta}$ with $x = 0.10$, the estimated magnetic volume fraction is 80% in the ground state. The SC volume fraction was estimated from the recovery of the electronic specific heat coefficient in the ground state by the application of magnetic field. It was at least 60%, suggesting the coexistence of the SC and short-range magnetically ordered regions in the sample. Numerically, a part of the short-range magnetically ordered regions appear to be spatially overlapped with the SC regions. However, it is plausible that the short-range magnetically ordered and SC regions are phase-separated, because the volume fraction of the short-range magnetically ordered region might be overestimated due to electronic dipole fields extending to the paramagnetic SC region.

The Cu-spin dynamics was further investigated by NMR using our reduced SC T'-samples by Yamamoto et al. [56] and Fukazawa [57]. As shown in Figure 6, the temperature dependence of $T_1 T$, where $1/T_1$ is the ^{63}Cu nuclear spin-lattice relaxation rate exhibited the Curie-Weiss behavior in a wide temperature range for $\text{Pr}_{1.3-x}\text{La}_{0.7}\text{Ce}_x\text{CuO}_{4+\delta}$ with $x = 0.10$ and 0.15, suggesting the existence of strong AF fluctuations in the underdoped and overdoped T'-cuprates. For the undoped (Ce-free) $\text{La}_{1.8}\text{Eu}_{0.2}\text{CuO}_{4+\delta}$, the bulk superconductivity was evidenced by the significant decrease in the Knight shift below T_c and AF fluctuations were observed in the normal state from the temperature dependence of $1/T_1$. These results suggest that AF fluctuations are related to the formation of electron pairs in the T'-cuprates as well as in the hole-doped cuprates.

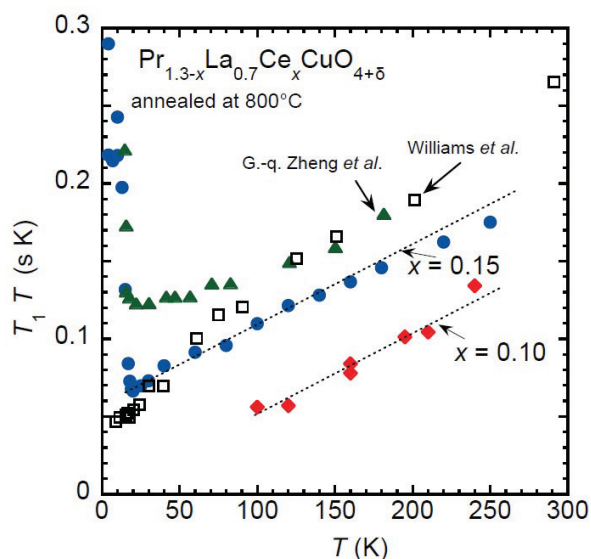


Figure 6. Temperature dependence of $T_1 T$ for reduced SC $\text{Pr}_{1.3-x}\text{La}_{0.7}\text{Ce}_x\text{CuO}_{4+\delta}$ with $x = 0.10$ and 0.15. Quoted from [56].

5. Superconducting Pairing Symmetry

While the SC pairing symmetry in the hole-doped cuprates is widely recognized to be d -wave, it is controversial in the electron-doped T'-cuprates. Early studies of impurity effects in $\text{Nd}_{2-x}\text{Ce}_x\text{Cu}_{1-y}(\text{Zn},\text{Ni})_y\text{O}_4$ with $x = 0.15$ revealed that T_c was depressed by the magnetic impurity Ni much more rapidly than by the nonmagnetic impurity Zn [58]. This is typical of conventional s -wave superconductors. On the contrary, ARPES [50,59] and penetration depth [60] experiments etc. insisted the occurrence of d -wave superconductivity in $\text{Nd}_{2-x}\text{Ce}_x\text{CuO}_{4+\delta}$ with $x = 0.15$ and $\text{Pr}_{2-x}\text{Ce}_x\text{CuO}_{4+\delta}$

with $x = 0.15$. To clarify the SC pairing symmetry of the undoped (Ce-free) superconductivity in the T'-cuprates, impurity effects on T_c were precisely investigated in $\text{La}_{1.8}\text{Eu}_{0.2}\text{Cu}_{1-y}(\text{Zn,Ni})_y\text{O}_{4+\delta}$ [23]. Figure 7 displays the impurity-concentration dependence of T_c normalized by T_c of $y = 0$ $T_c^{y=0}$ in $\text{La}_{1.8}\text{Eu}_{0.2}\text{Cu}_{1-y}(\text{Zn,Ni})_y\text{O}_{4+\delta}$ together with the preceding results of T'-cuprates [58] and hole-doped $\text{La}_{2-x}\text{Sr}_x\text{Cu}_{1-y}(\text{Zn,Ni})_y\text{O}_4$ [58,61,62]. Obviously, the depression of T_c is almost the same between the Zn and Ni substitution in contrast to the preceding results of $\text{Nd}_{2-x}\text{Ce}_x\text{Cu}_{1-y}(\text{Zn,Ni})_y\text{O}_{4+\delta}$ with $x = 0.15$ [58]. Moreover, the change of $T_c/T_c^{y=0}$ in $\text{La}_{1.8}\text{Eu}_{0.2}\text{Cu}_{1-y}(\text{Zn,Ni})_y\text{O}_{4+\delta}$ follows the results of $\text{La}_{2-x}\text{Sr}_x\text{Cu}_{1-y}(\text{Zn,Ni})_y\text{O}_4$ in the optimally doped $x = 0.15$ and overdoped $x = 0.20$. Therefore, in $\text{La}_{1.8}\text{Eu}_{0.2}\text{CuO}_{4+\delta}$, the depression of T_c by the Zn and Ni substitution is probably due to the pair-breaking effect and the SC pairing symmetry is d -wave mediated by spin fluctuations as in the case of the hole-doped cuprates. In fact, our μSR [22] and NMR [57] results also revealed strong spin fluctuations in $\text{La}_{1.8}\text{Eu}_{0.2}\text{CuO}_{4+\delta}$. The characteristic temperature dependence of $1/T_1$ observed in $\text{La}_{1.8}\text{Eu}_{0.2}\text{CuO}_{4+\delta}$ implies the existence of nodal lines in the SC gap, supporting the above statement of the d -wave superconductivity [57]. Moreover, optical studies in the SC thin film of Pr_2CuO_x with $x \simeq 4$ have suggested that the temperature dependence of the magnetic penetration depth λ exhibits the d -wave-like behavior [38]. In future, we will further investigate the SC pairing symmetry by the transverse-field μSR technique. Accumulating results of λ , inversely proportional to the SC carrier density, in electron-doped T'-cuprates [55,63–65] and infinite-layer cuprates [66] revealed that the T_c vs. λ relation seemed not to intersect the origin, which is contrary to the results of hole-doped cuprates suggesting the Bose–Einstein-condensation-like pairing mechanism [67].

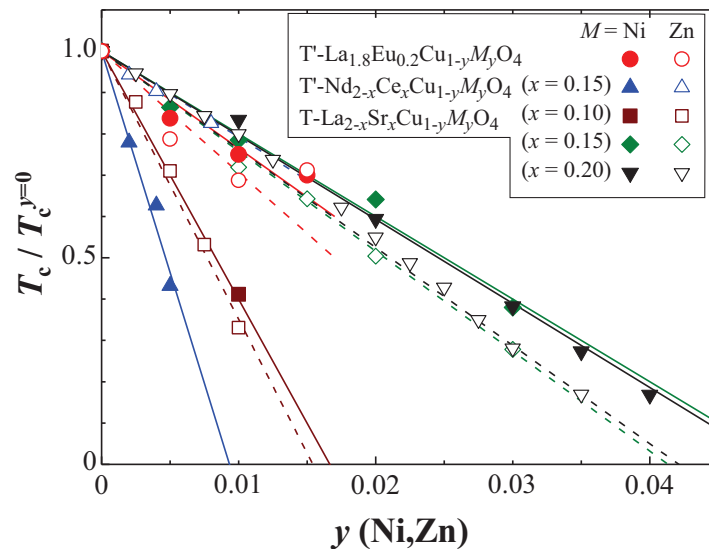


Figure 7. Impurity-concentration dependence of T_c normalized by T_c at $y = 0$ $T_c^{y=0}$ for undoped (Ce-free) $\text{La}_{1.8}\text{Eu}_{0.2}\text{Cu}_{1-y}(\text{Zn,Ni})_y\text{O}_{4+\delta}$ together with the preceding results of $\text{Nd}_{2-x}\text{Ce}_x\text{Cu}_{1-y}(\text{Zn,Ni})_y\text{O}_{4+\delta}$ ($x = 0.15$) [58] and of hole-doped $\text{La}_{2-x}\text{Sr}_x\text{Cu}_{1-y}(\text{Zn,Ni})_y\text{O}_4$ ($x = 0.10, 0.15, 0.20$) [58,61,62]. Filled and open symbols indicate data of the Ni and Zn substitution, respectively. Solid and dashed lines are guides to the eye.

6. Electronic Structure Model Based on the Strong Electron Correlation

Our transport and μSR results of $\text{Pr}_{1.3-x}\text{La}_{0.7}\text{Ce}_x\text{CuO}_{4+\delta}$ with $x = 0.10$ and $\text{La}_{1.8}\text{Eu}_{0.2}\text{CuO}_{4+\delta}$ revealed the following evolution of the electronic state through the reduction annealing. The ρ_{ab} showed that a strongly localized state of carriers in the as-grown sample changes to a metallic state with the Kondo effect in the reduced SC sample. The Hall resistivity of the reduced SC sample revealed the existence of multiple carriers. The μSR spectra revealed that, in the ground state, a long-range magnetic order of Cu spins in the as-grown sample changed to a short-range one coexisting with

the superconductivity in the reduced SC samples. It would be a reasonable speculation that an ideal T'-cuprate in which the excess oxygen is completely removed exhibits no AF order. The formation of the short-range magnetic order due to a very small amount of excess oxygen in the reduced SC sample suggests that the Cu spins are correlated with one another in the absence of excess oxygen in the ideal T'-cuprates. Therefore, the T'-cuprates exhibiting the undoped (Ce-free) superconductivity are regarded as strongly correlated electron systems as well as the hole-doped SC cuprates. Not the simple band-metal state without the electron correlation [39] but both the doublon-holon model [40], calculations using LDA with DMFT [41,42] and the two-particle self-consistent analysis [43] under the electron correlation would be able to explain the superconductivity in the undoped (Ce-free) and Ce-underdoped T'-cuprates.

The present transport and μ SR results are able to be understood in terms of the electronic structure model based on the strong electron correlation. The electronic structure models and schematic drawings of Cu spins and carriers in the CuO₂ plane are displayed in Figure 8a–c,e–g, respectively [21,22]. In the hole-doped high- T_c cuprates, the parent compounds are CT insulators as shown in Figure 8a characterized by the CT gap between UHB of the Cu $3d_{x^2-y^2}$ orbital and O $2p$ band. In the ideal undoped (Ce-free) T'-cuprates without excess oxygen shown in Figure 8c, on the other hand, the square-planar coordination of Cu and oxygen in the CuO₂ plane gives rise to a decrease in the Madelung energy of the Cu $3d$ orbitals compared with the octahedral coordination in the hole-doped cuprates. This brings about the lowering energy of UHB of the Cu $3d_{x^2-y^2}$ orbital, leading to the mixing of UHB with the Zhang-Rice singlet band. That is, the CT gap is collapsed, so that both mobile electrons and holes simultaneously emerge at the Fermi level in the parent compounds of the T'-cuprates, leading to the appearance of superconductivity without nominal doping of electrons by the Ce substitution. This is plausible, because the calculation of the Madelung energy results in a decrease in the energy of the Cu $3d$ orbitals by ~ 4 eV compared with the hole-doped cuprates with the CT gap ~ 2 eV [68]. In the case of excess oxygen residing adjacent to the CuO₂ plane, assuming that two holes are produced in the CuO₂ plane by one excess oxygen, the doped holes in the CuO₂ plane tend to be localized near the excess oxygen due to the disorder of the electrostatic potential. The holes are doped into the Cu $3d$ and O $2p$ orbitals taking into account the strong electron correlation. This is because the energy of the Cu $3d$ orbitals is raised by the excess oxygen due to increasing coordination number, as shown in Figure 8d. The doped hole in the Cu $3d$ orbital resides not in LHB of the Cu $3d_{x^2-y^2}$ orbital but in UHB of the Cu $3d_{3z^2-r^2}$ orbital in order to gain the energy of the Zhang-Rice singlet of Cu $3d_{x^2-y^2}$ (LHB) and O $2p$ spins. This is reasonable, because the splitting of Cu $3d_{x^2-y^2}$ and Cu $3d_{3z^2-r^2}$ in energy is smaller than the Mott-Hubbard gap of ~ 8 eV. Accordingly, Cu $3d_{3z^2-r^2}$ (LHB) free spins are probably induced at the Cu site adjacent to the excess oxygen. Both hole and electron carriers tend to be localized because of the disorder of the electrostatic potential near the excess oxygen, resulting in the recovery of the AF order of Cu $3d_{x^2-y^2}$ (LHB) spins. This is able to explain the increase in ρ_{ab} due to the strong localization and the hump of the temperature dependence of ρ_c due to the opening of the AF pseudogap.

In the CuO₂ plane in the as-grown non-SC samples of La_{1.8}Eu_{0.2}CuO_{4+ δ} and Pr_{1.3- x} La_{0.7}Ce _{x} CuO_{4+ δ} with $x = 0.10$, because of the moderate number of excess oxygen, carriers are strongly localized, as confirmed by ρ_{ab} [21], and the AF order is long-ranged, as illustrated in Figure 8e. In reduced SC La_{1.8}Eu_{0.2}CuO_{4+ δ} , as shown in Figure 8f, the CuO₂ plane should be mostly covered by short-range magnetically ordered regions, and superconductivity should appear around the boundary between the short-range magnetically ordered regions. In reduced SC Pr_{1.3- x} La_{0.7}Ce _{x} CuO_{4+ δ} with $x = 0.10$, because the amount of excess oxygen is smaller than that of reduced SC La_{1.8}Eu_{0.2}CuO_{4+ δ} , the short-range magnetically ordered regions decrease in correspondence to the increase in the SC volume fraction, as shown in Figure 8g. It is noted that the introduction of excess oxygen gives rise to free Cu spins of LHB of the Cu $3d_{3z^2-r^2}$ orbital in the CuO₂ plane just around itself, leading to the occurrence of the Kondo effect as confirmed by ρ_{ab} of reduced Pr_{1.3- x} La_{0.7}Ce _{x} CuO_{4+ δ} with $x = 0.10$ [21]. Accordingly, it is suggested that the short-range

magnetically ordered regions are formed around excess oxygen and superconductivity appears far from the excess oxygen.

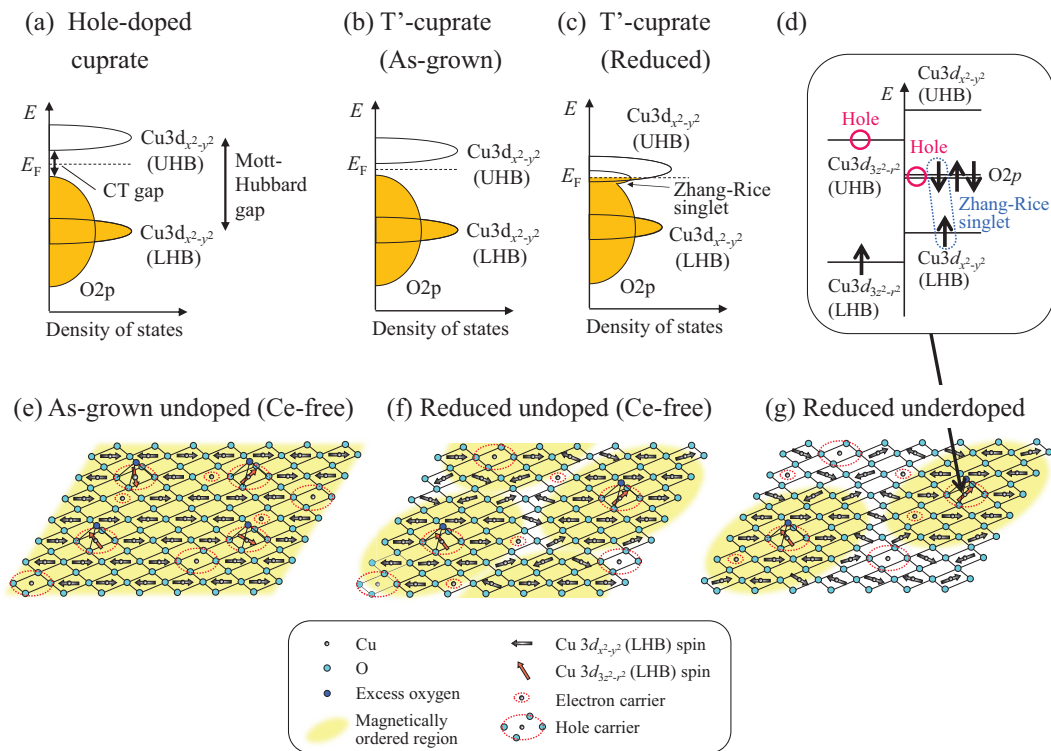


Figure 8. (a–c) Electronic structure models for (a) the parent compound of hole-doped high- T_c cuprate; (b) the as-grown undoped (Ce-free) T' -cuprate and (c) the reduced SC undoped (Ce-free) T' -cuprate. Arrows in (a) denote the charge-transfer (CT) and Mott-Hubbard gaps. (d) Electronic structure of the CuO_2 plane near the excess oxygen in undoped (Ce-free) T' -cuprates. (e–g) Schematic drawings of electron and hole carriers and Cu spins in the CuO_2 plane for (e) the as-grown non-SC undoped (Ce-free); (f) the reduced SC undoped (Ce-free) and (g) the reduced SC Ce-underdoped T' -cuprates.

As mentioned above, the ARPES experiment of $\text{Pr}_{1.3-x}\text{La}_{0.7}\text{Ce}_x\text{CuO}_{4+\delta}$ with $x = 0.10$ by Horio et al. [48] revealed that the AF pseudogap was closed on the whole Fermi surface, which is contrary to the former ARPES results in the T' -cuprates [49,50]. Considering both results of ARPES without the AF pseudogap and μSR with the short-range magnetic order, it is likely that Cu spins forming the short-range magnetic order have tiny magnetic moments. That is, the reduction annealing gives rise to not only the change of the long-range AF order to the short-range one but also the reduction of the magnetic moments of Cu spins, which is compatible with the decrease in the internal magnetic field at the muon site estimated from μSR results [22].

7. Future Issues

The present transport and μSR results of the undoped (Ce-free) and Ce-underdoped T' -cuprates uncovered that the superconductivity appeared under the strong electron correlation as in the case of the hole-doped cuprates. Here we discuss remaining unsolved issues of the T' -cuprates.

One is that the oxygen dynamics through the reduction annealing must be directly clarified. To date, several candidates of effects of the reduction annealing have been proposed; the removal of excess oxygen at the apical site [26,27], filling up Cu deficiencies [29,30], etc. Our crystal of $\text{Pr}_{1.3-x}\text{La}_{0.7}\text{Ce}_x\text{CuO}_{4+\delta}$ with $x = 0.10$ seems to be the case of the reduction of excess oxygen. Intriguing in our results is that the introduction of Cu vacancies into SC $\text{La}_{1.8}\text{Eu}_{0.2}\text{Cu}_{1-y}\text{O}_{4+\delta}$ does not change T_c so much up to $y = 0.015$ [23], which seems to be incompatible with the Cu-deficiency model.

In any case, this issue would be clarified by the recent high resolution neutron and X-ray diffraction experiments. Another issue is about carriers in the undoped (Ce-free) SC T'-cuprates. Our proposed electronic structure model indicates the presence of both electron and hole carriers, which is compatible with the present and former [53] Hall resistivity and NMR [54] results suggesting the existence of multiple carriers. On the other hand, the ARPES results shown in Figure 4 in $\text{Pr}_{1.3-x}\text{La}_{0.7}\text{Ce}_x\text{CuO}_{4+\delta}$ with $x = 0.10$ showed a hole-like Fermi surface without the AF pseudogap [48]. This is probably explained by considering that the overlapping UHB of the Cu $3d_{x^2-y^2}$ orbital and Zhang–Rice band form a mixing band in which both hole-like and electron-like carriers reside. The actual carrier concentration is also under debate. It has been suggested from the Hall effect results [69], etc. that the removal of excess oxygen does not simply correspond to the electron doping. Intriguing is the estimation of the electron concentration from the Fermi-surface volume observed in ARPES that T_c is unchanged in a wide electron concentration range in $\text{Pr}_{1.3-x}\text{La}_{0.7}\text{Ce}_x\text{CuO}_{4+\delta}$ [48]. On the contrary, very recent ARPES results in $\text{Pr}_{1-x}\text{LaCe}_x\text{CuO}_{4+\delta}$ revealed that T_c exhibited a parabolic change against the electron concentration estimated from the Fermi-surface volume [70].

The hole doping into the parent compounds of the T'-cuprates is an interesting way to clarify the electronic structure. Based on the proposed electronic structure model, the parent compounds of the T'-cuprates are no longer reference materials and T_c might continue to increase with hole doping into the parent compounds. Takamatsu et al. reported that the hole doping by the Sr/Ca substitution for La in $\text{La}_{1.8-x}\text{Eu}_{0.2}(\text{Ca},\text{Sr})_x\text{CuO}_{4+\delta}$ results in the decrease in T_c [19,71]. As Zn/Ni impurity effects on T_c in $\text{La}_{1.8}\text{Eu}_{0.2}\text{Cu}_{1-y}(\text{Zn},\text{Ni})_y\text{O}_{4+\delta}$ suggest that the electronic state of the parent compounds is similar to the overdoped regime of the hole-doped cuprates [23], it may be natural that further hole doping results in the decrease in T_c .

Acknowledgments: Our works were done in collaboration with Yosuke Mori, Akira Takahashi, Takuya Konno, Taro Ohgi, Tomohisa Takamatsu, Kensuke M. Suzuki, Koki Ohashi, Malik Angelh Baqiya, Koshi Kurashima, Masatsune Kato, Isao Watanabe, Masanori Miyazaki, Akihiro Koda and Ryosuke Kadono. Our works were supported by JSPS KAKENHI Grant Number 23540399 and 23108004 and by Sophia University Special Grant for Academic Research.

Author Contributions: Tadashi Adachi and Takayuki Kawamata conceived, designed and performed the experiments; Tadashi Adachi wrote the paper; Yoji Koike is responsible for the research. All authors have read and approved the final manuscript.

Conflicts of Interest: The authors declare no conflict of interest

References

- Schilling, A.; Cantoni, M.; Guo, J.D.; Ott, H.R. Superconductivity above 130 K in the Hg-Ba-Ca-Cu-O system. *Nature (Lond.)* **1993**, *363*, 56–58.
- Ren, Z.A.; Che, G.C.; Dong, X.L.; Yang, J.; Lu, W.; Yi, W.; Shen, X.L.; Li, Z.C.; Sun, L.L.; Zhou, F.; et al. Superconductivity and phase diagram in iron-based arsenic-oxides $\text{ReFeAsO}_{1-\delta}$ (Re = rare-earth metal) without fluorine doping. *Europhys. Lett.* **2008**, *83*, 17002.
- Drozdov, A.P.; Erements, M.I.; Troyan, I.A.; Ksenofontov, V.; Shylin, S.I. Conventional superconductivity at 203 Kelvin at high pressures in the sulfur hydride system. *Nature* **2015**, *525*, 73–76.
- Birgeneau, R.J.; Stock, C.; Tranquada, J.M.; Yamada, K. Magnetic neutron scattering in hole-doped cuprate superconductors. *J. Phys. Soc. Jpn.* **2006**, *75*, 111003.
- Watanabe, I.; Adachi, T.; Takahashi, K.; Yairi, S.; Koike, Y.; Nagamine, K. Muon-spin-relaxation study of the effect of nonmagnetic impurities on the Cu-spin fluctuations in $\text{La}_{2-x}\text{Sr}_x\text{Cu}_{1-y}\text{Zn}_y\text{O}_4$ around $x = 0.115$. *Phys. Rev. B* **2002**, *65*, 180516.
- Adachi, T.; Yairi, S.; Takahashi, K.; Koike, Y.; Watanabe, I.; Nagamine, K. Muon spin relaxation and magnetic susceptibility studies of the effects of nonmagnetic impurities on the Cu spin dynamics and superconductivity in $\text{La}_{2-x}\text{Sr}_x\text{Cu}_{1-y}\text{Zn}_y\text{O}_4$ around $x = 0.115$. *Phys. Rev. B* **2004**, *69*, 184507.
- Risdiana; Adachi, T.; Oki, N.; Yairi, S.; Tanabe, Y.; Omori, K.; Koike, Y.; Suzuki, T.; Watanabe, I.; Koda, A.; et al. Cu spin dynamics in the overdoped regime of $\text{La}_{2-x}\text{Sr}_x\text{Cu}_{1-y}\text{Zn}_y\text{O}_4$ probed by muon spin relaxation. *Phys. Rev. B* **2008**, *77*, 054516.

8. Adachi, T.; Oki, N.; Risdiana; Yairi, S.; Koike, Y.; Watanabe, I. Effects of Zn and Ni substitution on the Cu spin dynamics and superconductivity in $\text{La}_{2-x}\text{Sr}_x\text{Cu}_{1-y}(\text{Zn,Ni})_y\text{O}_4$ ($x = 0.15\text{--}0.20$): Muon spin relaxation and magnetic susceptibility study. *Phys. Rev. B* **2008**, *78*, 134515.
9. Koike, Y.; Adachi, T. Impurity and magnetic field effects on the stripes in cuprates. *Physica C* **2012**, *481*, 115–124.
10. Kopp, A.; Ghosal, A.; Chakravarty, S.S. Competing ferromagnetism in high-temperature copper oxide superconductors. *Proc. Natl. Acad. Sci. USA* **2007**, *104*, 6123–6127.
11. Barbiellini, B.; Jarlborg, T. Importance of local band effects for ferromagnetism in hole-doped La_2CuO_4 cuprate superconductors. *Phys. Rev. Lett.* **2008**, *101*, 157002.
12. Jia, C.J.; Nowadnick, E.A.; Wohlfeld, K.; Kung, Y.F.; Chen, C.C.; Johnston, S.; Tohyama, T.; Moritz, B.; Devereaux, T.P. Persistent spin excitations in doped antiferromagnets revealed by resonant inelastic light scattering. *Nat. Commun.* **2014**, *5*, 3314.
13. Sonier, J.E.; Kaiser, C.V.; Pacradouni, V.; Sabok-Sayr, S.A.; Cochrane, C.; MacLaughlin, D.E.; Komiya, S.; Hussey, N.E. Direct search for a ferromagnetic phase in a heavily overdoped nonsuperconducting copper oxide. *Proc. Natl. Acad. Sci. USA* **2010**, *107*, 17131–17134.
14. Kurashima, K.; Adachi, T.; Suzuki, K.M.; Fukunaga, Y.; Kawamata, T.; Noji, T.; Koike, Y. Possible ferromagnetic phase in non-superconducting heavily overdoped cuprates of Bi-2201 . *J. Phys. Conf. Ser.* **2014**, *568*, 022003.
15. Tokura, Y.; Takagi, H.; Uchida, S. A superconducting copper oxide compound with electrons as the charge carriers. *Nature* **1989**, *337*, 345–347.
16. Yamada, K.; Kurahashi, K.; Uefuji, T.; Fujita, M.; Park, S.; Lee, S.H.; Endoh, Y. Commensurate spin dynamics in the superconducting state of an electron-doped cuprate superconductor. *Phys. Rev. Lett.* **2003**, *90*, 137004.
17. Tsukada, A.; Krockenberger, Y.; Noda, M.; Yamamoto, H.; Manske, D.; Alff, L.; Naito, M. New class of T' -structure cuprate superconductors. *Solid State Commun.* **2005**, *133*, 427–431.
18. Asai, S.; Ueda, S.; Naito, M. Superconductivity in bulk T' - $(\text{La,Sm})_2\text{CuO}_4$ prepared via a molten alkaline hydroxide route. *Physica C* **2011**, *471*, 682–685.
19. Takamatsu, T.; Kato, M.; Noji, T.; Koike, Y. Undoped and hole-doped superconductors T' - $\text{La}_{1.8-x}\text{Eu}_{0.2}\text{Sr}_x\text{CuO}_4$ ($x = 0$ and 0.05) prepared by solid-state reaction. *Appl. Phys. Express* **2012**, *5*, 073101.
20. Matsumoto, O.; Utsuki, A.; Tsukada, A.; Yamamoto, H.; Manabe, T.; Naito, M. Generic phase diagram of “electron-doped” T' cuprates. *Physica C* **2009**, *469*, 924–927.
21. Adachi, T.; Mori, Y.; Takahashi, A.; Kato, M.; Nishizaki, T.; Sasaki, T.; Kobayashi, N.; Koike, Y. Evolution of the electronic state through the reduction annealing in electron-doped $\text{Pr}_{1.3-x}\text{La}_{0.7}\text{Ce}_x\text{CuO}_{4+\delta}$ ($x = 0.10$) single crystals: Antiferromagnetism, Kondo effect, and superconductivity. *J. Phys. Soc. Jpn.* **2013**, *82*, 063713.
22. Adachi, T.; Takahashi, A.; Suzuki, K.M.; Baqiya, M.A.; Konno, T.; Takamatsu, T.; Watanabe, I.; Koda, A.; Miyazaki, M.; Kadono, R.; et al. Strong electron correlation behind the superconductivity in Ce-free and Ce-underdoped high- T_c T' -cuprates. *J. Phys. Soc. Jpn.* **2016**, *85*, 114716.
23. Ohashi, K.; Kawamata, T.; Takamatsu, T.; Adachi, T.; Kato, M.; Koike, Y. Pairing symmetry studied from impurity effects in the undoped superconductor T' - $\text{La}_{1.8}\text{Eu}_{0.2}\text{CuO}_4$. *J. Phys. Soc. Jpn.* **2016**, *85*, 093703.
24. Armitage, N.P.; Fournier, P.; Greene, R.L. Progress and perspectives on electron-doped cuprates. *Rev. Mod. Phys.* **2010**, *82*, 2421–2487.
25. Fournier, P. T' and infinite-layer electron-doped cuprates. *Physica C* **2015**, *514*, 314–338.
26. Radaelli, P.G.; Jorgensen, J.D.; Schultz, A.J.; Peng, J.L.; Greene, R.L. Evidence of apical oxygen in Nd_2CuO_y determined by single-crystal neutron diffraction. *Phys. Rev. B* **1994**, *49*, 15322.
27. Schultz, A.J.; Jorgensen, J.D.; Peng, J.L.; Greene, R.L. Single-crystal neutron-diffraction structures of reduced and oxygenated $\text{Nd}_{2-x}\text{Ce}_x\text{CuO}_y$. *Phys. Rev. B* **1996**, *53*, 5157.
28. Xu, X.Q.; Mao, S.N.; Jiang, W.; Peng, J.L.; Greene, R.L. Oxygen dependence of the transport properties of $\text{Nd}_{1.78}\text{Ce}_{0.22}\text{CuO}_{4\pm\delta}$. *Phys. Rev. B* **1996**, *53*, 871.
29. Mang, P.K.; Larochelle, S.; Mehta, A.; Vajk, O.P.; Erickson, A.S.; Lu, L.; Buyers, W.J.L.; Marshall, A.F.; Prokes, K.; Greven, M. Phase decomposition and chemical inhomogeneity in $\text{Nd}_{2-x}\text{Ce}_x\text{CuO}_{4\pm\delta}$. *Phys. Rev. B* **2004**, *70*, 094507.
30. Kang, H.J.; Dai, P.; Campbell, B.J.; Chupas, P.J.; Rosenkranz, S.; Lee, P.L.; Huang, Q.; Li, S.; Komiya, S.; Ando, Y. Microscopic annealing process and its impact on superconductivity in T' -structure electron-doped copper oxides. *Nat. Mater.* **2007**, *6*, 224–229.

31. Kimura, H.; Noda, Y.; Sato, F.; Tsuda, K.; Kurahashi, K.; Uefuji, T.; Fujita, M.; Yamada, K. X-ray and electron diffraction study of a precipitation phase in $\text{Nd}_{1.85}\text{Ce}_{0.15}\text{CuO}_{4+y}$ single crystal. *J. Phys. Soc. Jpn.* **2005**, *74*, 2282–2286.
32. Luke, G.M.; Le, L.P.; Sternlieb, B.J.; Uemura, Y.J.; Brewer, J.H.; Kadono, R.; Kiefl, R.F.; Kreitzman, S.R.; Riseman, T.M.; Stronach, C.E.; et al. Magnetic order and electronic phase diagrams of electron-doped copper oxide materials. *Phys. Rev. B* **1990**, *42*, 7981–7988.
33. Fujita, M.; Kubo, T.; Kuroshima, S.; Uefuji, T.; Kawashima, K.; Yamada, K.; Watanabe, I.; Nagamine, K. Magnetic and superconducting phase diagram of electron-doped $\text{Pr}_{1-x}\text{LaCe}_x\text{CuO}_4$. *Phys. Rev. B* **2003**, *67*, 014514.
34. Tranquada, J.M.; Sternlieb, B.J.; Axe, J.D.; Nakamura, Y.; Uchida, S. Evidence for stripe correlations of spins and holes in copper oxide superconductors. *Nature* **1995**, *375*, 561–563.
35. Fujita, M.; Matsuda, M.; Lee, S.H.; Nakagawa, M.; Yamada, K. Low-energy spin fluctuations in the ground states of electron-doped $\text{Pr}_{1-x}\text{LaCe}_x\text{CuO}_{4+\delta}$ cuprate superconductors. *Phys. Rev. Lett.* **2008**, *101*, 107003.
36. Brinkmann, M.; Rex, T.; Bach, H.; Westerholt, K. Extended superconducting concentration range observed in $\text{Pr}_{2-x}\text{Ce}_x\text{CuO}_{4-\delta}$. *Phys. Rev. Lett.* **1995**, *74*, 4927–4930.
37. Krockenberger, Y.; Irie, H.; Matsumoto, O.; Yamagami, K.; Mitsuhashi, M.; Tsukada, A.; Naito, M.; Yamamoto, H. Emerging superconductivity hidden beneath charge-transfer insulators. *Sci. Rep.* **2013**, *3*, 2235.
38. Chanda, G.; Lobo, R.P.S.M.; Schachinger, E.; Wosnitza, J.; Naito, M.; Pronin, A.V. Optical study of superconducting Pr_2CuO_x with $x \simeq 4$. *Phys. Rev. B* **2014**, *90*, 024503.
39. Massidda, S.; Hamada, N.; Yu, J.; Freeman, A.J. Electronic structure of Ne-Ce-Cu-O, A Fermi liquid superconductor. *Physica C* **1989**, *157*, 571–574.
40. Yokoyama, H.; Ogata, M.; Tanaka, Y. Mott transitions and *d*-wave superconductivity in half-filled-band Hubbard model on square lattice with geometric frustration. *J. Phys. Soc. Jpn.* **2006**, *75*, 114706.
41. Das, H.; Saha-Dasgupta, T. Electronic structure of La_2CuO_4 in the T and T' crystal structures using dynamical mean field theory. *Phys. Rev. B* **2009**, *79*, 134522.
42. Weber, C.; Haule, K.; Kotliar, G. Strength of correlations in electron- and hole-doped cuprates. *Nat. Phys.* **2010**, *6*, 574–578.
43. Ogura, D.; Kuroki, K. Asymmetry of superconductivity in hole- and electron-doped cuprates: Explanation within two-particle self-consistent analysis for the three-band model. *Phys. Rev. B* **2015**, *92*, 144511.
44. Risdiana; Adachi, T.; Oki, N.; Koike, Y.; Suzuki, T.; Watanabe, I. Muon spin relaxation study of the Cu spin dynamics in electron-doped high- T_c superconductor $\text{Pr}_{0.86}\text{LaCe}_{0.14}\text{Cu}_{1-y}\text{Zn}_y\text{O}_4$. *Phys. Rev. B* **2010**, *82*, 014506.
45. Onose, Y.; Taguchi, Y.; Ishizaka, K.; Tokura, Y. Charge dynamics in underdoped $\text{Nd}_{2-x}\text{Ce}_x\text{CuO}_4$: Pseudogap and related phenomena. *Phys. Rev. B* **2004**, *69*, 024504.
46. Sun, X.F.; Kurita, Y.; Suzuki, T.; Komiyama, S.; Ando, Y. Thermal conductivity of $\text{Pr}_{1.3-x}\text{La}_{0.7}\text{Ce}_x\text{CuO}_4$ single crystals and signatures of stripes in an electron-doped cuprate. *Phys. Rev. Lett.* **2004**, *92*, 047001.
47. Sekitani, T.; Naito, M.; Miura, N. Kondo effect in underdoped n-type superconductors. *Phys. Rev. B* **2003**, *67*, 174503.
48. Horio, M.; Adachi, T.; Mori, Y.; Takahashi, A.; Yoshida, T.; Suzuki, H.; Ambolode, L.C.C., II; Okazaki, K.; Ono, K.; Kumigashira, H.; et al. Suppression of the antiferromagnetic pseudogap in the electron-doped high-temperature superconductor by protect annealing. *Nat. Commun.* **2016**, *7*, 10567.
49. Armitage, N.P.; Ronning, F.; Lu, D.H.; Kim, C.; Damascelli, A.; Shen, K.M.; Feng, D.L.; Eisaki, H.; Shen, Z.X.; Mang, P.K.; et al. Doping dependence of an n-type cuprate superconductor investigated by angle-resolved photoemission spectroscopy. *Phys. Rev. Lett.* **2002**, *88*, 257001.
50. Matsui, H.; Terashima, K.; Sato, T.; Takahashi, T.; Wang, S.C.; Yang, H.B.; Ding, H.; Uefuji, T.; Yamada, K. Angle-resolved photoemission spectroscopy of the antiferromagnetic superconductor $\text{Nd}_{1.87}\text{Ce}_{0.13}\text{CuO}_4$: Anisotropic spin-correlation gap, pseudogap, and the induced quasiparticle mass enhancement. *Phys. Rev. Lett.* **2005**, *94*, 047005.
51. Da Silva Neto, E.H.; Comin, R.; He, F.; Sutarto, R.; Jiang, Y.; Greene, R.L.; Sawatzky, G.A.; Dacascelli, A. Charge ordering in the electron-doped superconductor $\text{Nd}_{2-x}\text{Ce}_x\text{CuO}_4$. *Science* **2015**, *347*, 282–285.
52. Dagan, Y.; Qazilbash, M.M.; Hill, C.P.; Kulkarni, V.N.; Greene, R.L. Evidence for a quantum phase transition in $\text{Pr}_{2-x}\text{Ce}_x\text{CuO}_{4-\delta}$ from transport measurements. *Phys. Rev. Lett.* **2004**, *92*, 167001.
53. Li, P.; Barakirev, F.F.; Greene, R.L. High-field Hall resistivity and magnetoresistance of electron-doped $\text{Pr}_{2-x}\text{Ce}_x\text{CuO}_{4-\delta}$. *Phys. Rev. Lett.* **2007**, *99*, 047003.

54. Jurkatat, M.; Rybicki, D.; Sushkov, O.P.; Williams, G.V.M.; Erb, A.; Haase, J. Distribution of electrons and holes in cuprate superconductors as determined from ^{17}O and ^{63}Cu nuclear magnetic resonance. *Phys. Rev. B* **2014**, *90*, 140504.
55. Kojima, K.M.; Krockenberger, Y.; Yamauchi, I.; Miyazaki, M.; Hiraishi, M.; Koda, A.; Kadono, R.; Kumai, R.; Yamamoto, H.; Ikeda, A.; et al. Bulk superconductivity in undoped T' - $\text{La}_{1.9}\text{Y}_{0.1}\text{CuO}_4$ probed by muon spin rotation. *Phys. Rev. B* **2014**, *89*, 180508.
56. Yamamoto, M.; Kohori, Y.; Fukazawa, H.; Takahashi, A.; Ohgi, T.; Adachi, T.; Koike, Y. Existence of large antiferromagnetic spin fluctuations in Ce-doped T' -cuprate Superconductors. *J. Phys. Soc. Jpn.* **2016**, *85*, 024708.
57. Fukazawa, H. Chiba University, Chiba, Japan. Personal communication, 2017.
58. Tarascon, J.M.; Wang, E.; Kivelson, S.; Bagley, B.G.; Hull, G.W.; Ramesh, R. Magnetic versus nonmagnetic ion substitution effects on T_c in the La-Sr-Cu-O and Nd-Ce-Cu-O systems. *Phys. Rev. B* **1990**, *42*, 218.
59. Sato, T.; Kamiyama, T.; Takahashi, T.; Kurahashi, K.; Yamada, K. Observation of $d_{x^2-y^2}$ -like superconducting gap in an electron-doped high-temperature superconductor. *Science* **2001**, *291*, 1517.
60. Kokales, J.D.; Fournier, P.; Mercaldo, L.V.; Talanov, V.V.; Greene, R.L.; Anlage, S.M. Microwave electrodynamic of electron-doped cuprate superconductors. *Phys. Rev. Lett.* **2000**, *85*, 3696–3699.
61. Sreedhar, K.; Metcalf, P.; Honig, J. Effect of a change in the carrier concentration and disorder on the superconducting transition temperature of the $\text{La}_{2-x}\text{Sr}_x\text{Cu}_{1-y}\text{Ni}_y\text{O}_4$ system. *Physica C* **1994**, *227*, 160–168.
62. Uchida, S. Zn-impurity effects on high-temperature superconductivity. *Physica C* **2001**, *357*, 25–29.
63. Homes, C.C.; Clayman, B.P.; Peng, J.L.; Greene, R.L. Optical properties of $\text{Nd}_{1.85}\text{Ce}_{0.15}\text{CuO}_4$. *Phys. Rev. B* **1997**, *56*, 5525.
64. Nugroho, A.A.; Sutjahja, I.M.; Rusydi, A.; Tjia, M.O.; Menovsky, A.A.; de Boer, F.R.; Franse, J.J.M. Reversible magnetization of a $\text{Nd}_{1.85}\text{Ce}_{0.15}\text{CuO}_{4-\delta}$ single crystal. *Phys. Rev. B* **1999**, *60*, 15384.
65. Homes, C.C.; Lobo, R.P.S.M.; Fournier, P.; Zimmers, A.; Greene, R.L. Optical determination of the superconducting energy gap in electron-doped $\text{Pr}_{1.85}\text{Ce}_{0.15}\text{CuO}_4$. *Phys. Rev. B* **2006**, *74*, 214515.
66. Satoh, K.H.; Takeshita, S.; Koda, A.; Kadono, R.; Ishida, K.; Pyon, S.; Sasagawa, T.; Takagi, H. Fermi-liquid behavior and weakly anisotropic superconductivity in the electron-doped cuprate $\text{Sr}_{1-x}\text{La}_x\text{CuO}_2$. *Phys. Rev. B* **2008**, *77*, 224503.
67. Uemura, Y.J. Superfluid density of high- T_c cuprate systems: Implication on condensation mechanisms, heterogeneity and phase diagram. *Solid State Commun.* **2003**, *126*, 23–28.
68. Tsukada, A.; Shibata, H.; Noda, M.; Yamamoto, H.; Naito, M. Charge transfer gap for T' - RE_2CuO_4 and T - La_2CuO_4 as estimated from Madelung potential calculations. *Physica C* **2006**, *445*, 94–96.
69. Gauthier, J.; Gagné, S.; Renaud, J.; Gosselin, M.-É.; Fournier, P.; Richard, P. Difference roles of cerium substitution and oxygen reduction in transport in $\text{Pr}_{2-x}\text{Ce}_x\text{CuO}_4$ thin films. *Phys. Rev. B* **2007**, *75*, 024424.
70. Song, D.; Han, G.; Kyung, W.; Seo, J.; Cho, S.; Kim, B.S.; Arita, M.; Shimada, K.; Namatame, H.; Taniguchi, M.; et al. Electron number-based phase diagram of $\text{Pr}_{1-x}\text{La}_x\text{Ce}_x\text{CuO}_{4-\delta}$ and possible absence of disparity between electron- and hole-doped cuprate phase diagram. *Phys. Rev. Lett.* **2017**, *118*, 137001.
71. Takamatsu, T.; Kato, M.; Noji, T.; Koike, Y. Superconductivity in hole-doped $\text{La}_{1.8-x}\text{Eu}_{0.2}\text{Ca}_x\text{CuO}_4$ with the Nd_2CuO_4 -type structure. *Phys. Procedia* **2014**, *58*, 46–49.

